

## RESEARCH ARTICLE



WILEY

# Constant innervation despite pubertal growth of the mouse penis

Leopold Purkart<sup>1</sup> | Johanna Sigl-Glöckner<sup>1</sup> | Michael Brecht<sup>1,2</sup>

<sup>1</sup>Bernstein Center for Computational Neuroscience Berlin, Humboldt-Universität zu Berlin, Berlin, Germany

<sup>2</sup>NeuroCure Cluster of Excellence, Humboldt-Universität zu Berlin, Berlin, Germany

## Correspondence

Michael Brecht, Bernstein Center for Computational Neuroscience Berlin, Humboldt-Universität zu Berlin, Philippstrasse 13, Haus 6, Berlin, Germany.  
Email: michael.brecht@bccn-berlin.de

## Funding information

Deutsche Forschungsgemeinschaft, Grant/Award Number: BR 3479/11-1

## Peer Review

The peer review history for this article is available at <https://publons.com/publon/10.1002/cne.24892>.

## Abstract

The sexual characteristics of the vertebrate body change under the control of sex hormones. In mammals, genitals undergo major changes in puberty. While such bodily changes have been well documented, the associated changes in the nervous system are poorly understood. To address this issue, we studied the growth and innervation of the mouse penis throughout puberty. To this end, we measured length and thickness of the mouse penis in prepubertal (3–4 week old) and adult (8–10 week old) mice and performed fiber counts of the dorsal penile nerve. We obtained such counts with confocal imaging of proximal sections of the mouse penis after paraffin embedding and antibody staining against Protein-Gene-Product-9.5 or Neurofilament-H in combination with antigen retrieval procedures. We find that the mouse penis grows roughly 1.4 times in both thickness and length. Fiber counts in the dorsal penile nerve were not different in prepubertal ( $1,620 \pm 165$  fibers per penis) and adult ( $1,572 \pm 383$  fibers per penis) mice, however. Antibody staining along with myelin staining by Luxol-Fast-Blue suggested about 57% of penile nerve fibers were myelinated. Quantification of the area of mouse somatosensory penis cortex allowed us to compare cortical magnification of the penile cortex and the whisker-barrel-cortex systems. This comparison suggested that 2 to 4 times less cortical area is devoted to a penile-nerve-fiber than to a whisker-nerve-fiber. The constant innervation of mouse penis through puberty suggests that the pubertal increase of cortical magnification of the penis is not simply a reflection of peripheral change.

## KEYWORDS

mouse penis, myelin, nerve fibers, puberty, RRID:AB\_11212161, RRID:AB\_2336227, RRID:AB\_2534096, RRID:AB\_2535792, RRID:AB\_2622233, RRID:AB\_2534016, RRID:SCR\_001622, RRID:SCR\_003070, somatosensory cortex

## 1 | INTRODUCTION

During puberty, the external genitals undergo significant morphological and physiological changes which can easily be assessed by the external inspection of the body (Han & Lee, 2014; Tomova et al., 2010). Beyond physical maturation, the pubertal surge in sex hormones also controls the sexual differentiation of the brain (Juraska,

Sisk, & DonCarlos, 2013; Schulz & Sisk, 2016). Therefore, the neurohumoral mechanisms that control puberty have been intensely investigated (Terasawa & Kurian, 2012). Interestingly, it has been shown that puberty is not simply a rigid, age-dependent developmental program; instead puberty is in mammals heavily influenced by social cues (Bronson & Maruniak, 1975; Lenschow, Sigl-Glöckner, & Brecht, 2017; Levin & Johnston, 1986; Vandenbergh, 1983): the smell of male

This is an open access article under the terms of the Creative Commons Attribution-NonCommercial License, which permits use, distribution and reproduction in any medium, provided the original work is properly cited and is not used for commercial purposes.

© 2020 The Authors. *The Journal of Comparative Neurology* published by Wiley Periodicals, Inc.

urine (Drickamer & Murphy, 1978; Mucignat-Caretta, Caretta, & Cavaggioni, 1995) or tactile cues such as genital touch (Lenschow et al., 2017) can powerfully advance the sexual maturation of rodents. Besides advancing the physical maturation, recent studies have shown that puberty also changes the central representation of the genitals in primary somatosensory cortex. After identifying the genital field in primary somatosensory using anatomical methods combined with microelectrode mapping (Lenschow et al., 2016), it was shown that this area undergoes a significant expansion during puberty, not only in rats but also in other mammals (Lauer, Lenschow, & Brecht, 2017; Lenschow et al., 2016; Lenschow et al., 2017).

This observation was highly unusual, because the topographic map in layer 4 of primary somatosensory cortex is conceived as particularly stable (Feldman & Brecht, 2005; Glazewski & Fox, 1996). It raises the question, what determines the size of different body parts within primary somatosensory cortex. Typically, the size of the cortical field is proportional to the density of nerve fibers innervating the peripheral surface. Accordingly, the more richly innervated body parts occupy larger shares of cortical surface resulting in an afferent magnification of the body part. In rodents for example, the representation of the whisker pad occupies the majority of the primary somatosensory cortex (Lee & Woolsey, 1975; Welker & Van der Loos, 1986). Given this relationship and the pubertal expansion of genital cortex, we wondered whether there is a concurrent increase in the number of nerve fibers innervating the sex organs.

We decided to address this question in male mice, for which we have already analyzed pubertal changes in genital cortex (Lauer et al., 2017; Sigl-Glöckner et al., 2019). In males, genital cortex receives input from the dorsal nerve of the penis (Calaresu, 1970), which is a branch of the pudendal nerve and runs centrally along the dorsal surface of the penis, superior to the cavernous bodies. It contains mainly sensory fibers providing afferent sensory signals to the brain and some motor fibers for contracting muscles during erection. This somatic (sensory and motor) innervation is critical for sexual function (Chen et al., 2018; Larsson & Södersten, 1973; Weech & Ashurst, 2019). The autonomic innervation of the penis on the other hand is mainly provided by the cavernous nerves, which control neurovascular events during erection. However, staining with nitric oxide synthase has suggested that the dorsal penile nerve does also contain some autonomic fibers (Carrier et al., 1995), yet these seem to be mainly located at the penile helium (Colombel, Droupy, Paradis, Lassau, & Benoît, 1999). As a result, the dorsal penile nerve is considered as containing mostly sensory afferents that relay sensory input to the skin of the penis to the brain. Whether the density of these fibers changes during puberty is however still unknown.

In our current analysis we therefore investigate the mouse dorsal penile nerve and specifically asked the following questions: (a) What procedure should be applied to reveal and count individual nerve fibers in the mouse penis? (b) How many nerve fibers are in the mouse dorsal penile nerve in prepubertal and adult animals? (c) What is the relationship between fibers in the dorsal penile nerve and the cortical area representing the penis in the brain?

## 2 | MATERIALS AND METHODS

### 2.1 | Animals

All experimental procedures were performed according to German guidelines on animal welfare under the supervision of local ethics committees. Prepubertal and adult C57BL/6JRj mice were purchased from Janvier Labs (St Berthevin Cedex, France) and perfused within 1 day upon arrival. Prepubertal mice were 3 weeks of age and adult mice were between 6 and 10 weeks of age. We ensured, that in no prepubertal males balanopreputial separation had already occurred. For measuring the size of the primary somatosensory cortex, we purchased adult transgenic animals that express crecrecombinase in cortical layer 4 (Scnn1a-Tg3-Cre, #009613) and Ai9-reporter mice (#007909) mice from Jackson Labs and crossed those lines. The resulting offspring constitutionally expresses the fluorescent marker tdTomato in excitatory neurons of cortical layer 4. Animals were killed under permits T0078/16 and T0215/18.

### 2.2 | Penile tissue preparation

Mice were anesthetized with isoflurane and injected with an overdose of urethane (20%, 1 ml/100 g). Subsequently, animals were transcardially perfused with phosphate buffer, followed by a 4% paraformaldehyde (PFA) solution and genitals were removed, cleaned from connective tissue and stored in a 4% PFA solution for ~24 hr. Depending on the protocol, the solution was then changed to 30% sucrose for frozen sections or 70% ethanol for paraffin embedding. Frozen sections were cut at 40  $\mu$ m on a Frigomobil (Leica) and kept free floating in 0.1 M phosphate buffer saline (PBS).

For paraffin embedding, penises were cut into halves and put into a 20% ethylenediaminetetraacetic acid (EDTA) solution (EDTA-Entkalkungslösung ~20%, pH 7.4, Morphisto, Art. Nr. 13,412) for ~7 days for decalcification. This step dissolves the baculum to avoid it damaging sections during slicing. Subsequently, the tissue was transferred to a Leica TP 1020 tissue processor, running an ascending alcohol series (Table 1). Next, penises were kept in a furnace at 60°C for 24 hr and embedded in paraffin blocks using the Leica HistoCore Arcadia H. Blocks were cut into 16  $\mu$ m sections, which were left to floated in a 45°C preheated water-bath. The sections were then mounted on Thermo Scientific Superfrost Ultra Plus® slides, dried on a warming plate at 35°C and stored overnight in a furnace at 42°C. Before applying the immunohistochemistry protocol, sections were deparaffinized and rehydrated in a descending ethanol series (Table 2).

### 2.3 | Penile size measurement

To measure penile length, we horizontally aligned dissected penises right after preparation to a millimeter scale. The mouse penis varies in diameter along the proximal-distal as well as dorsal-ventral axis. Therefore, we quantified the diameter by measuring the width of

**TABLE 1** Dehydration program Leica TP 1020 for penile tissue sections

Step	Reagent	Vacuum	Duration
1	80% ethanol	N	1 hr
2	90% ethanol	Y	2 hr
3	96% ethanol	Y	1 hr
4	96% ethanol	Y	1 hr
5	96% ethanol	Y	1 hr
6	100% ethanol	Y	2 hr
7	100% ethanol	Y	2 hr
8	100% ethanol	Y	2 hr
9	Neo-clear (xylene substitute)	Y	2 hr
10	Neo-clear (xylene substitute)	Y	2 hr
11	Paraffin	Y	3 hr
12	Paraffin	Y	5 hr

Note: Y = yes, N = no.

**TABLE 2** Deparaffinization und rehydration protocol for penile tissue sections

Step	Reagent	Duration
1	Xylene	5 min
2	Xylene	5 min
3	100% ethanol	3 min
4	100% ethanol	3 min
5	96% ethanol	1 min
6	80% ethanol	1 min
7	60% ethanol	1 min
8	Running cold tap water	3–5 min

three paraffin-embedded cross-sections (proximal, medial, and distal) per penis using the ImageJ and calculated the mean.

## 2.4 | Brain tissue preparation

Some experiments were conducted in layer 4 transgenic reporter mice (Scnn1a x Ai9) to measure the size of the primary somatosensory cortex. Brains were removed, hemispheres were separated, subcortical brain areas removed and cortices were flattened between two glass slides separated by clay spacers. Glass slides were weighed down with small ceramic weights for 3 hr. Afterwards, flattened cortices were left free floating in 4% PFA overnight. On the next day, slices were transferred in a 30% sucrose solution for cryoprotection. Afterwards, 40  $\mu$ m sections were cut using a Frigomobil (Leica) and sections were mounted on gelatin coated glass slides.

## 2.5 | Immunohistochemical staining

For immunohistochemical staining of penile tissue, we performed heat induced epitope retrieval (HIER) using a citrate buffer (Antigen

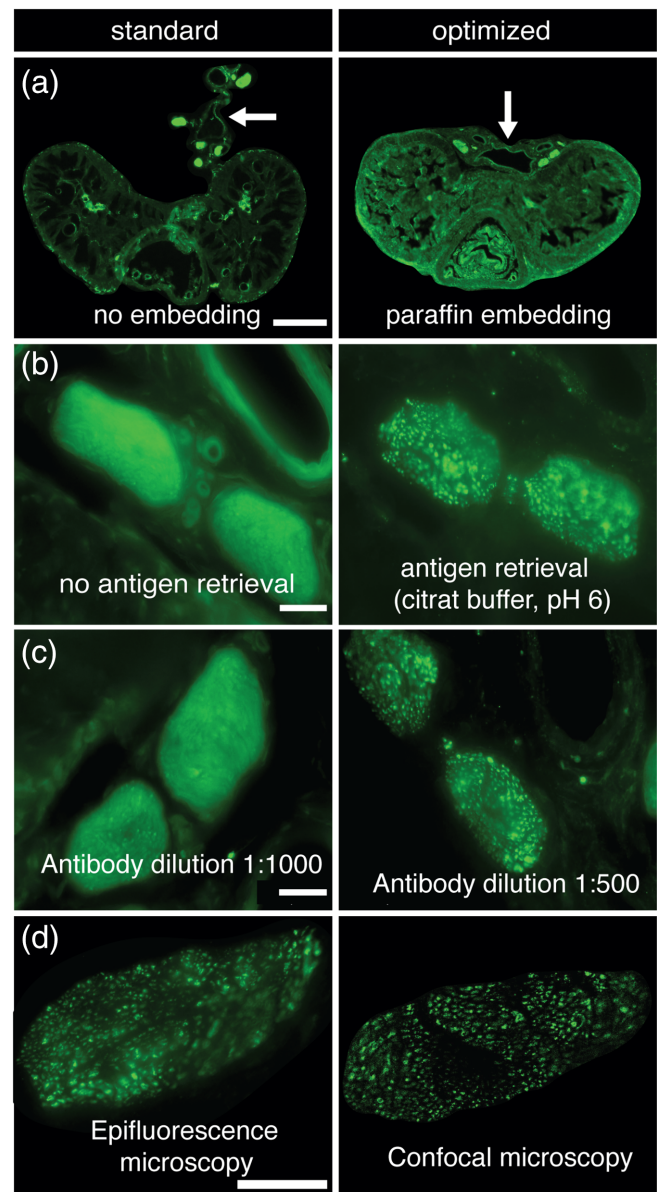


**FIGURE 1** Protocol development for dorsal penile nerve fiber counts based on protein gene product (PGP) 9.5 antibody staining of the mouse penis ( $n = 7$ ). (a) Left, proximal cross section of an adult mouse penis, which was not embedded. Anatomical structures are poorly preserved. The intercrural septum (arrows) is almost completely detached from the corpora cavernosa (CC). Urethra and the surrounding cavernous bodies are dislocated. Right, section cut after paraffin embedding. Structures are well preserved and in their correct anatomical position. Scale bar = 400  $\mu$ m. (b) Left, nerve bundles of the dorsal nerve of the penis stained without antigen retrieval. Detailed structures within the bundles are not discernible. Scale bar = 30  $\mu$ m. Right, same as left panel, but following antigen retrieval using citrate buffer. Note the clearly visible single fibers within the bundles of the dorsal nerve of the penis. (c) Same as (b), but using different antibody dilutions. Left, dilution of 1:1,000 was not sufficient to stain single fibers within bundles of the dorsal nerve of the penis. Right, dilution of 1:500 reveals single fibers. Scale bar = 30  $\mu$ m. (d) Left, An epifluorescence micrograph of a single dorsal nerve of the penis bundle. Due to high background fluorescence the image appears blurry. Scale bar = 40  $\mu$ m. Right, same as left, but the micrograph was acquired using a confocal microscope

Unmasking Solution, Citric Acid Based, pH 6, 100× concentrated stock solution, Vector Laboratories Cat# H-3301, RRID:AB\_2336227). A water-bath with a staining dish, containing the antigen retrieval solution, was preheated to 95–100°C. Mounted sections were placed in the dish, heated for ~60 min and left to cool for 30 min at room temperature. For free-floating sections, it was not necessary to perform HIER so that we could continue with immunohistochemistry. Antibody staining was performed according to standard procedures. In summary, penis sections were pre-incubated for an hour at room temperature in a blocking solution (0.1 M PBS, 2.5% Bovine Serum Albumin and 0.5% Triton X-100). Afterwards, primary antibodies were diluted in a solution containing 0.5% Triton X-100 and 1% Bovine Serum Albumin. We prepared nerve fiber stains with primary antibodies against either PGP 9.5 or Neurofilament H as specified below; both antibody stains led to complete and fully analyzable staining patterns of the dorsal penile nerve. Accordingly, results from both antibodies were pooled and entered our analysis of nerve fiber counts. The primary antibodies against PGP 9.5 (Rabbit polyclonal, Agilent Cat# Z5116, RRID:AB\_2622233,  $n = 4$  penises) and Neurofilament H (Chicken polyclonal, Millipore Cat# AB5539, RRID:AB\_11212161,  $n = 12$  penises) were incubated for at least 48 hr under gentle agitation at 4°C. Incubation with the primary antibodies was followed by detection with secondary antibodies, coupled to the fluorophores Alexa 488 (Donkey anti rabbit: Thermo Fisher Scientific Cat# A-21206, RRID:AB\_2535792; Goat anti chicken: Thermo Fisher Scientific Cat# A-11039, RRID:AB\_2534096) or Alexa 546 (Donkey anti rabbit: Thermo Fisher Scientific Cat# A10040, RRID:AB\_2534016). The secondary antibodies were diluted (1:1,000) in 1% Bovine Serum Albumin in 0.1 M PBS and the reaction was allowed to proceed overnight in the dark at 4°C. We mounted the free-floating frozen sections on Superfrost glass slides and covered them with Fluoromount G® (Biozol, Eching, Germany) mounting medium. The same was done for the already mounted, paraffin embedded sections.

## 2.6 | Microscopy

Z-stacks were taken on a Leica DM5500B epifluorescence microscope and on a Leica TCS SP5 confocal microscope with a 63× oil lens

(axial resolution 0.772  $\mu\text{m}$ ). The z-planes were 0.1  $\mu\text{m}$  and 1  $\mu\text{m}$  apart, respectively. The images obtained were 1,024 × 1,024 pixels in size with a field of view between 240 × 240  $\mu\text{m}$  and 55 × 55  $\mu\text{m}$ . For nerve fiber counts, high resolution images of 55 × 55  $\mu\text{m}$  were used. Stacks were analyzed using ImageJ (RRID:SCR\_003070).

## 2.7 | Analysis and statistics

Localization and analysis of nerve fiber counts is described in the following results section. Descriptive statistics were calculated in Excel and are expressed as mean ± standard deviation (STD). Data were tested for normality and compared using independent *t* tests in MATLAB (Mathworks, RRID:SCR\_001622).

## 2.8 | Optimization of a staining/imaging protocol for a dorsal penile nerve fiber counts

Our initial attempts to count nerve fibers in the mouse dorsal penile nerve failed. In particular, we encountered the following problems: (a) the baculum (the penis bone) would disrupt sectioning and impose the need for decalcification procedures. (b) Free floating tissue sections dissociated (Figure 1a, left), preventing the anatomical localization of the dorsal nerve of the penis. Specifically, the intercrural septum (IS), which contains blood vessels (dorsal vein (DV), dorsal arteries (DA)) and the bundles of the dorsal nerve of the penis completely detached from connective tissue. Therefore, we turned to paraffin embedding (Figure 1a, right), which maintained all anatomical structures very well. (c) During the embedding process antigens are chemically modified and masked. As a result, they can no longer be detected by antibodies and the signal to noise ratio staining was insufficient for nerve fiber counts (Figure 1b, left). Therefore, we had to perform antigen retrieval procedures, that is, we treated sections, mounted on highly adhesive slides, at 95°C in citrate buffer. Subsequent antibody staining nicely revealed single fibers within bundles of the DNP (Figure 1b, right). (d) Furthermore, we had to adjust the antibody concentration for optimal staining. An antibody dilution of 1:1,000 resulted in high background staining (Figure 1c, left). Hence, we employed antibody dilution of 1:500, which

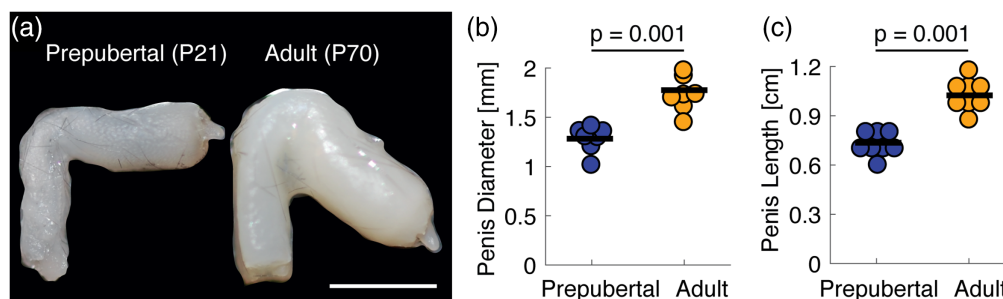


**FIGURE 2** Pubertal growth of the mouse penis. (a) Dissected penises of a prepubertal (P21, left) and an adult mouse (P70, right). The penises were dissected directly after perfusion and detached from connective tissue. Scale bar = 2 mm. (b) The mean diameter (black bar) of adult penises (orange,  $n = 8$ ) was larger than that of prepubertal penises (blue,  $n = 8$ ). (c) The mean length (black bar) of adult penises (orange,  $n = 8$ ) was also longer than that of prepubertal penises (blue,  $n = 8$ )

greatly improved the contrast (Figure 1c, right). (e) Finally, confocal microscopy (Figure 1d, right) was superior to standard epifluorescence microscopy (Figure 1d, left) in resolving single nerve fibers. To stain myelin sheaths in the dorsal penile nerve, we placed deparaffinized slides in 1% Luxol Fast Blue solution at 56°C for 24 hr followed by differentiation in 0.05% lithium carbonate.

## 2.9 | Measurement of cortical areas

To quantify the relationship between nerve fibers in the DNP and the cortical area representing the penis in primary somatosensory cortex, we analyzed the brains of transgenic mice, which expressed tdTomato in the cortical input layer 4 (the Scnn1a mouse line). The expression in this mouse line is limited to areas receiving strong lemniscal input, and therefore nicely reveals the somatotopy of the somatosensory cortex. We then identified the subfield representing the genitals by superimposing the Scnn1a/tdTomato layer 4 map with functional signals from *in vivo* Ca-imaging or intrinsic imaging of sensory responses to genital stimulation (Sigl-Glöckner et al., 2019). We also identified C2 whisker barrel based on the known topography of the barrel field.

## 3 | RESULTS

### 3.1 | Size measurements of prepubertal and adult mouse penises

First, we assessed the overall appearance of pre- and post-pubertal mouse penises. Prepubertal mice were 3 weeks of age, while adult mice were around 8 weeks. Overall, prepubertal and adult penises were similar in appearance (Figure 2a). However, adult penises were both, wider (mean diameter: 1.3 mm ± 0.1 mm (prepubertal) versus 1.8 mm ± 0.2 mm (adult),  $X^2 = 10.89$ ,  $p = .001$ , Figure 2b) and longer (mean length: 7.3 mm ± 0.7 mm (prepubertal) versus 10.5 mm ± 0.9 mm (adult),  $X^2 = 11.29$ ,  $p = .001$ , Figure 2c). These measurements refer only to flaccid, dissected penises and we have no information about the effects of puberty on erected penises. We conclude that there is a major size increase of the mouse penis in puberty.

### 3.2 | Identification of dorsal penile nerve in the mouse penis

To identify the course of the dorsal penile nerve along the proximodistal extent of the mouse penis, we stained tissue sections with the pan-neuronal markers Protein Gene Product 9.5 (PGP 9.5, Figure 3). We took fluorescent micrographs along the proximo-distal axis of the penis (Figure 3a). Proximal to the body, the corpora cavernosa were largest and surrounded the intercrural septum ventrally and laterally so that all nerve bundles were close to the midline (Figure 3b, left). The urethra and the associated cavernous body were arranged at the ventral end of the section. A closer look at the intercrural septum shows the well-marked dorsal

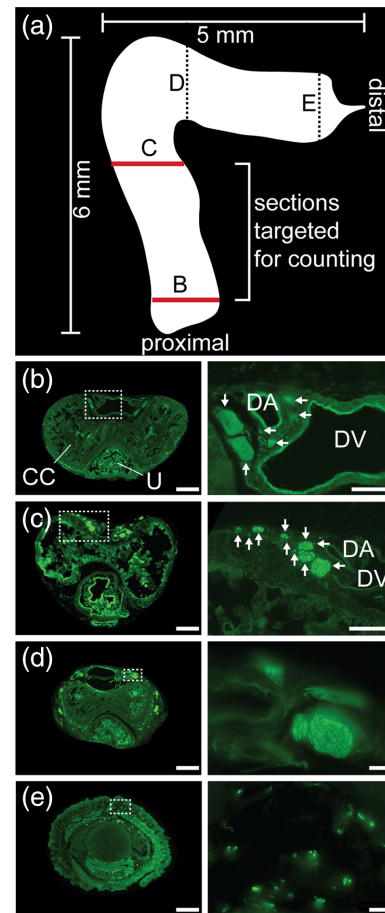


**FIGURE 3** Localization of the dorsal penile nerve along the proximal-distal axis of the mouse penis ( $n = 3$ ). (a) Schematic drawing of the mouse penis. Dashed and red lines indicate the approximate positions of the cross-sections shown in b to e. (b) Left, proximal penis cross-section. The corpora cavernosa (CC) are slightly bent dorsally and surround the intercrural septum laterally, urethra (U). Right, inset of intercrural septum with dorsal vein, dorsal arteries and bundles of the dorsal nerve of the penis (arrows). Bundles are always located left and right of the dorsal vein. (c) Note that the intercrural septum is more flattened than in (b) and laterally elongated. Right panel: dorsal vein and dorsal arteries are constricted and dorsal nerve of the penis branches out. (d) Left, corpora cavernosa are decreased in size and nerve bundles are migrating laterally. Right, only few bundles are left in the area of the intercrural septum. (e) Distal section. Left, baculum covering the center with lateral leftovers of the corpora cavernosa. Urethra is flattened. Right, no bundles of the dorsal nerve of the penis are left. Single fibers of various nerves are visible. Scale bars = 300  $\mu$ m (left column), 150  $\mu$ m (b), 150  $\mu$ m (c), 25  $\mu$ m (d), and 25  $\mu$ m (e)

vein, one dorsal artery and several bundles of the dorsal nerve of the penis (Figure 3b, white arrows, right). More distally, some of the smaller dorsal penile nerve bundles spread lateral of the intercrural septum (Figure 3c, left) and the dorsal vein diameter was reduced (Figure 3c, right). Even more distal sections (Figure 3d, left) showed nerve bundles further lateral that approached the ventral side of the penis. Furthermore, additional single nerve fibers appeared within the corpora cavernosa, which in turn were considerably decreased in size. In the intercrural

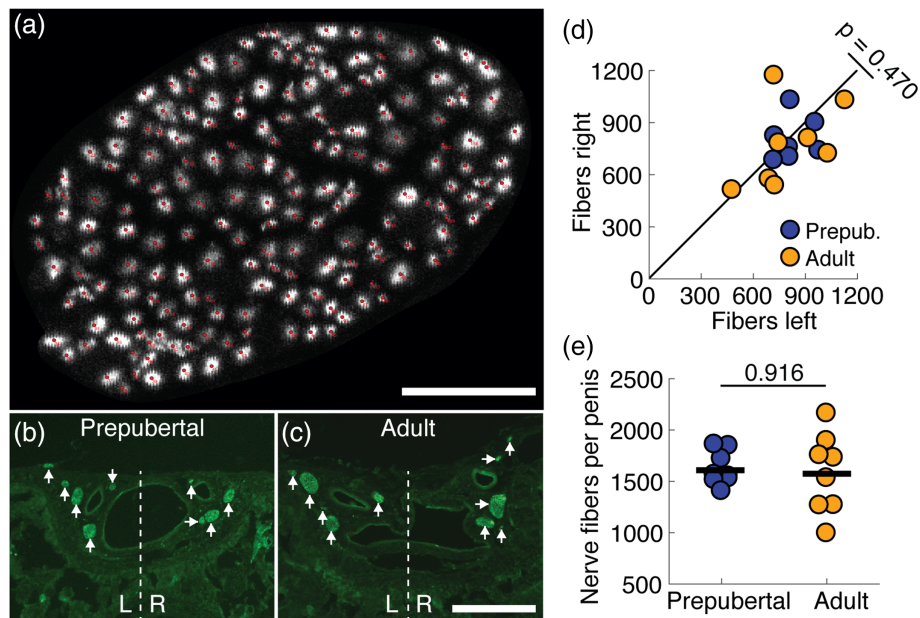


**FIGURE 4** Nerve fiber counts are bilaterally symmetric and the same in prepubertal and adult mouse dorsal penile nerve sections. (a) Confocal micrograph of dorsal nerve of the penis bundle of male aged P56. Nerve fibers were stained with a primary antibody against Neurofilament H and visualized using a secondary antibody conjugated to Alexa Fluor 488. Red dots mark single fibers, that were counted. Scale bar = 15  $\mu$ m. (b) Cross-section through the dorsal part of an adult penis stained as described in (a). The intercrural septum is subdivided in left and right, bundles of the DNP (arrows) are clearly visible on each side. (c) Same as (b), but for a prepubertal penis (from a P21 animal). Scale bar = 300  $\mu$ m. (d) The fiber distribution on the left and right side of the mouse penis. There is no significant difference ( $p = .470$ ). There is a correlation between the fiber count of both sides ( $r = .44$ ) with no significant difference ( $p = .089$ ).  $n = 8$  each. (e) There is no significant ( $p = .916$ ) difference between the mean number of fibers within bundles of the dorsal nerve of the penis between prepubertal (blue) and adult (orange) animals ( $n = 8$  each)

septum, there were few nerve bundles left, while some fibers appeared (Figure 3d, right). The very distal part of the penis appears almost devoid of nerve bundles. Instead, it is densely covered with single fibers (Figure 3e, right). The center is filled with the baculum, which is laterally surrounded by the diminishing corpora cavernosa (Figure 3e, left) (Phillips, Wright, Gradie, Johnston, & Pask, 2015). The canal of the urethra is compressed and horizontally elongated. In these more distal regions (Figure 3a,d,e), the dorsal penile nerve branches out and mingles with other nerve fibers from the cavernous nerve and the perineal nerve. Here, single bundles belonging to the dorsal penile nerve can no longer be identified. Similar to the description of Chen et al. (2018), we find that proximal to the body, the dorsal nerve of the penis is compact in the area of the intercrural septum (Figure 3a). We conclude that in the proximal penis, the dorsal nerve of the penis consisted of four to five main bundles on each side of the dorsal vein, which are easily and reliably identified and well suited for quantification.

### 3.3 | Single nerve fiber counts

Using pan-neuronal antibody staining (PGP 9.5 or Neurofilament H), we were able to reveal single nerve fibers within each bundle, which we captured using confocal microscopy (Figure 4a, red dots). Single fibers were counted in z-stacks. Bundles located outside of the intercrural septum were not considered as part of the dorsal penile nerve and were therefore

excluded. Hence, we identified the main bundles of the dorsal nerve of the penis (Figure 4b,c) in sections of prepubertal and adult penises. Usually, there were two to four large ones, containing more than 100 fibers and two to four small ones with 10 to 100 fibers. All bundles were located lateral to the dorsal vein, so a subdivision by side was easy to make (Figure 4b,c). The number of nerve fibers was similar between left and right side in both, prepubertal and adult penises. Figure 4d shows counts for all bundles on the left and right side, for both, prepubertal and adult penises, the fiber count between both sides was weakly but not significantly correlated ( $r = .44$ ,  $p = .089$  n.s.). Next, we compared the overall number of fibers in all bundles of the dorsal nerve of the penis in eight prepubertal and eight adult males. In order to avoid confounds owing to suboptimal staining, anatomical irregularities or damaged tissue, we counted in three sections within the proximal penis region identified in Figure 3a and derived the mean for each animal. Overall, different sections had similar numbers of fibers for the same mouse. To assess the variance of nerve fiber counts within animals, we normalized individual counts. Normalization was performed by dividing individual nerve fiber counts by the mean nerve fiber count and computing the standard deviation of the resulting values across animals. We find that compared to the mean (by definition 1) the standard deviation of fiber counts within animals was  $\pm 0.15$ . However, there was no difference in the number of nerve fibers within the dorsal penile nerve between prepubertal and adult mouse penises (Figure 4e, mean fiber number:  $1620 \pm 165$  (prepubertal) versus  $1,572 \pm 383$  (adult),  $\chi^2 = 0.04$ ,  $p = .916$ ). We conclude that the

innervation of the mouse penis as measured by dorsal penile nerve fiber counts does not change during puberty.

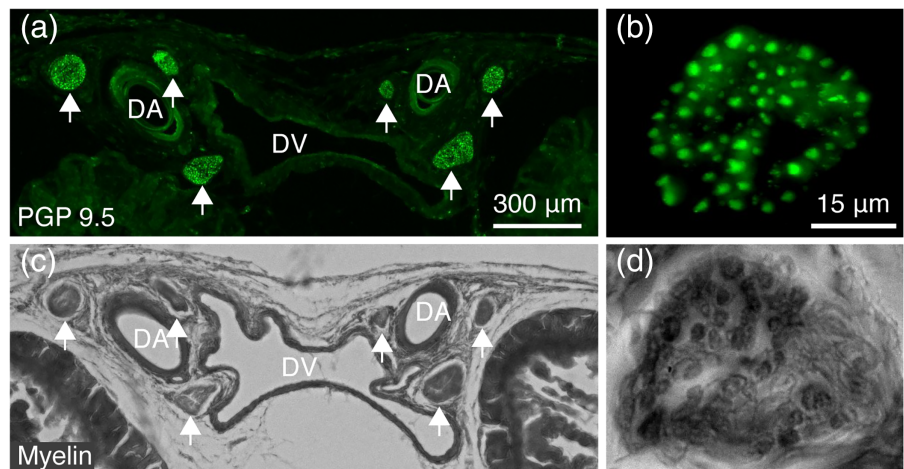
### 3.4 | Myelination of the dorsal penile nerve fibers

Most previous work on peripheral nerve fiber counts focused on counts of myelin sheets. To compare our antibody based counts of—presumably—all nerve fibers to this earlier work, we obtained counts of antibody stained fibers (Figure 5a,b) and of myelinated fibers (Figure 5c,d) in alternating sections. Specifically, we visualized myelin sheets by Luxol Fast Blue staining (Figure 5d). As expected PGP-positive fibers and myelin sheets appeared in similar position but there were also PGP-positive fibers that lacked myelin sheets (Figure 5b,d). Next, we quantified PGP-positive fibers and counts of myelin sheets (Figure 5e). We counted nerve fibers within the same nerve bundles ( $n = 16$ ) in adjacent sections (as identified by dense PGP or Luxol Fast Blue staining) in three animals and found that on average 57% of all fibers within one bundle of the dorsal nerve of the penis are myelinated (Figure 5e). We conclude that nerve fiber counts

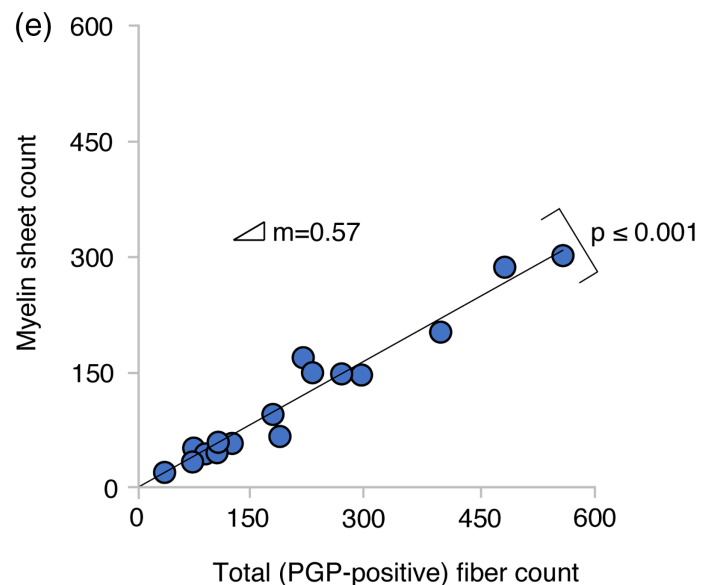
based solely on myelin staining likely underestimate nerve fiber counts of the dorsal penile nerve.

### 3.5 | Cortical magnification of penile and whisker nerve fibers

Sensory signals from the body surface reach the cortex in the cortical input layer 4, which contains a topographic map of the body surface with corresponding subfields for different body parts. To compare the cortical area devoted to penile fibers to that of other peripheral fibers, such as the C2 barrel, we measured the size the cortical penis representation. To this end, we used a transgenic mouse line, expressing the red fluorescent marker tdTomato in Scnn1a-positive neurons. In somatosensory cortex Scnn1a expression is layer 4 specific and restricted to areas receiving strong thalamic input; hence, within cortical layer 4 such expression nicely reveals the somatotopy of the somatosensory cortex (Figure 6a). Using serial sections of flattened cortices, we reconstructed the full body map and focused our analysis of the genital cortex (orange) and the C2 barrel field (green,



**FIGURE 5** Myelination of the dorsal penile nerve fibers. (a) Cross-section of mouse penis stained with PGP 9.5 to visualize nerve fibers. Bundles (arrows), dorsal vein (DV) and dorsal arteries (DA) are clearly visible. (b) High magnification view of one bundle of the dorsal penile nerve stained with PGP 9.5. Single nerve fibers are visible. (c) Adjacent cross-section of same mouse penis as (a) but stained with Luxol Fast Blue to visualize myelin sheets. Bundles (arrows) of the dorsal penile nerve are the same in position and number. (d) Same bundle as in (b) but stained with Luxol Fast Blue myelin staining. Fewer myelin sheets than PGP positive nerve fibers (b) are visible. (e) x-y plot of total (PGP-positive) fiber count against myelin sheet (Luxol Fast Blue) counts from various penile nerve fiber bundles ( $n = 16$  from three animals). Myelin sheet and total fiber counts were strongly correlated ( $r = .98$ ) but significantly fewer myelin sheets than PGP-positive fibers were counted (paired  $t$  test), a regression line was fitted to the data has a slope of 0.57 slightly more than half of the dorsal penile nerve fibers are myelinated



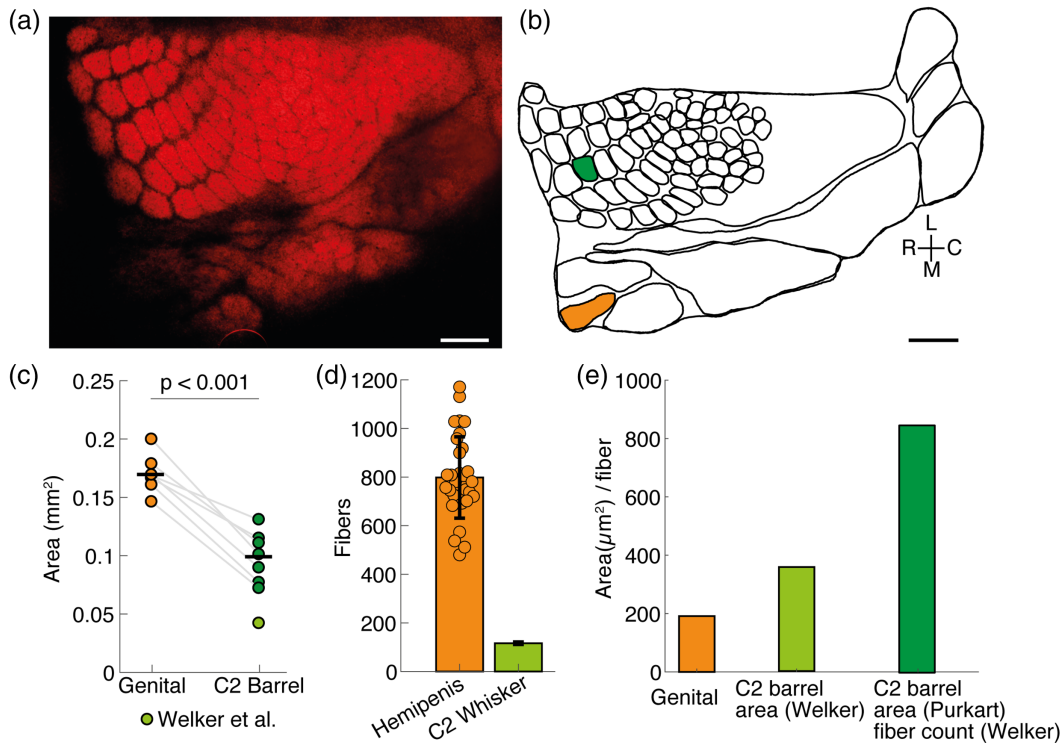


**FIGURE 6** Cortical magnification of whisker and penile fibers. (a) Flattened tangential section of a Scnn1a-Tg3-Cre x Ai9 mouse somatosensory cortex. Scnn1a + expression reveals the somatotopy of the somatosensory cortex within L4 of primary somatosensory cortex. Scale bar = 500  $\mu\text{m}$ . (b) Drawing through several serial tangential sections showing the complete somatotopy of the primary somatosensory cortex of the mouse. Cortical areas receiving peripheral inputs from the C2 whisker (green) and from the genital (orange) are highlighted. Scale bar = 500  $\mu\text{m}$ . (c) Cortical area devoted to the genital representation (orange, left,  $0.17 \pm 0.02 \text{ mm}^2$ ) is larger than the C2 barrel (right, green,  $0.10 \pm 0.02 \text{ mm}^2$ ) in mouse primary somatosensory cortex ( $n = 7$ ,  $p < .001$ ). Black bars indicate the mean. As a reference, the mean area of the C2 barrel from an unflattened mouse cortex as reported by Welker and Van der Loos (1986) is shown in light green. (d) The number of fibers counted in the dorsal nerve of 32 hemi-penises (left, orange,  $799 \pm 167$  fibers) and the mean number of fibers innervating the C2 whisker follicle ( $117 \pm 5$  fibers), data are replotted from Welker and Van der Loos (1986). (e) Cortical area ( $\mu\text{m}^2$ ) per nerve fiber for the genital (orange) and the C2 barrel (green). Light green: C2 barrel area estimate and C2 whisker fiber count by Welker and Van der Loos (1986). Dark green: C2 barrel area estimated by Purkart et al. divided by C2 whisker fiber count reported by Welker and Van der Loos (1986)

Figure 6b). Overall, genital cortex is larger than the C2 barrel ( $n = 7$  adult mice, genital:  $0.17 \pm 0.02 \text{ mm}^2$  vs. C2 barrel:  $0.10 \pm 0.02 \text{ mm}^2$ , Figure 6c). Our estimates of the C2 barrel field were larger than those previously reported by Welker and Van der Loos (1986), shown in light green. We believe that this discrepancy stems from substantial differences in the histological procedures. Specifically, the flattening of the cortical sheet is likely to result in an increase in the size of cortical areas. Next, we pooled the fiber counts for all 32 “hemi-penises” (half-penises) from 8 prepubertal and 8 adult mice and compared the results to the reported mean number of nerve fibers innervating the C2 barrel (Welker & Van der Loos, 1986). While a hemi-penis is innervated by  $799 \pm 167$ , the average C2 whisker follicle receives only  $117 \pm 5$  nerve fibers. Finally, we calculated ratio between the cortical area (in the tangential/horizontal plane) and the number of innervating fibers for the penis and the C2 whisker. Welker and Van der Loos (1986) also estimated this ratio (shown in light green). However, for a fairer comparison to our current results from the genital cortex, we think one needs to consider the larger barrel and genital size in our flattened cortices. Hence, we also calculated this ratio using our own estimate of C2 barrel field

size divided by the number of fibers counted by Welker and Van der Loos (1986), shown here in dark green. Our results suggest that the cortical area devoted to a peripheral fiber innervating the C2 barrel is larger compared to the cortical area devoted to a peripheral fiber innervating the penis. Overall, the afferent cortical magnification of C2 whisker fiber is  $\sim 2$  to 4 times larger than that of a dorsal penile nerve fiber.

#### 4 | DISCUSSION

We found that the mouse penis grows substantially in puberty. We developed a methodology, which allows resolving and counting single nerve fibers in the mouse dorsal penile nerve. Our nerve fiber counts revealed a bilaterally symmetric innervation of the mouse penis, which does not change in puberty. We also show that about 57% of nerve fibers innervating the penis are myelinated. Finally, we suggest that the somatosensory cortical area receiving peripheral inputs from a dorsal penile nerve fiber is smaller, compared to the cortical area receiving input from a whisker follicle nerve fiber.

Our methodology combined a variety of conventional techniques such as decalcification, antibody staining with the pan-neuronal markers PGP-9.5 or Neurofilament H, antigen retrieval and paraffin embedding. This approach allowed reliably identifying the proximodistal course and architecture of the mouse dorsal penile nerve. We found dorsal penile nerve consists of several sub-bundles on each side of the intercrural septum. Our observations confirm the description of Chen et al. (2018), but contrast with the picture generally conveyed by text-books, where the dorsal nerve of the penis is invariably depicted as a single bundle running bilateral to the dorsal vein. Furthermore, the branching of the dorsal nerve of the penis appears similar in both, pre- and post-pubertal mice with no visible morphological differences. Our methodology also allowed the quantitative analysis of penile innervation in the mouse with single fiber resolution.

We found that the adult mouse penis is symmetrically innervated and that the mouse dorsal penile nerve contains about 1,600 fibers per penis. Our data on fiber numbers in sub-bundles appear to be similar to those counted by other authors (Chen et al., 2018). This total fiber count is similar and slightly higher than counts of myelinated fibers in dorsal penis nerve obtained from adult rats, where 1,423 myelinated fibers in total were counted (Calaresu, 1970). The most obvious explanation for the larger number of fibers in our study on the mouse penis than in the Calaresu study on the rat penis is that our antibody stains detected a large fraction of un-myelinated fibers, which were not detectable in the osmium stains performed by Calaresu (1970). This interpretation is substantiated by our dual antibody (PGP) based fiber counts and assessment of myelin sheets (stained by Luxol Fast Blue) in adjacent sections (Figure 5). These data indicate that only about 57% of fibers, positive for the pan neuronal marker PGP 9.5, are also myelinated. Thus, it appears likely that mice have a lower dorsal penile nerve fiber count than rats as expected from the differences in body size. The only other study we could find on dorsal penile nerve fiber counts comes from rhesus monkeys. In rhesus monkeys a higher nerve fiber count (3,200–5,600 myelinated fibers per penis) was reported (Herbert, 1973). This rhesus monkey number is clearly higher than the nerve fiber counts observed by us in the mouse. Still, also this difference (a factor of ~2.5) is remarkably small if one considers the approximately ~100× larger body weight of rhesus monkeys compared to mice. Optic nerves fiber counts of mouse (~64,000, Honjin, Sakato, & Yamashita, 1977) and rhesus monkey (~1,600,000; Sandell & Peters, 2001) differ by a factor of 25. These considerations suggest the possibility that the number of dorsal penile nerve fibers is relatively similar across species. This is a very preliminary conclusion, however, and we need more information about dorsal penile nerve fiber numbers. In particular, it would be worth determining dorsal penile nerve fiber counts in humans, who have a quite specialized sex life and no baculum (Diamond, 2018).

Our data also show that there is no difference in the number of nerve fibers within the dorsal penile nerve between prepubertal and adult male mice. While our data argue against major changes in penile innervation during puberty in mice, they do not totally rule out this possibility. Our analysis focused on the proximal penis, where the dorsal penile nerve is rather compact. Within the dorsal nerve of the

penis, there are sympathetic, parasympathetic and sensory fibers, expressing the neuropeptides/transmitters tyrosine hydroxylase (TH), neural nitric oxide synthase (nNOS) and calcitonin gene-related peptide (CGRP), respectively (Chen et al., 2018). Sympathetic and sensory fibers originate from the pudendal nerve, whereas parasympathetic fibers originate from the cavernous nerve (Colombel et al., 1999; Rea, 2016; Yucel & Baskin, 2003). Puberty associated remodeling of genital innervation might be associated with certain subtypes of sensory fibers. It has been shown, that after nerve crushing, there is a decrease in parasympathetic fibers that are contributed by the cavernous nerve to the dorsal nerve of the penis. Therefore, peripheral nerve damage can lead to selective plasticity of fiber subtypes within the dorsal penile nerve. Given that the length of the prepuce changes during puberty, it is possible more distal nerve branches do exhibit puberty dependent plasticity. Such observations have also been made in female rodents, where the density and sensitivity of sensory axons has been shown to be modulated by the estrous cycle and repeated vaginocervical stimulation (Adler, Davis, & Komisaruk, 1977; Conde & Komisaruk, 2012; Liao & Smith, 2011; Zoubina, Fan, & Smith, 1998). The authors quantified the relative density of distributed, single axons in the vaginal wall. In contrast to them, we counted fibers in the region of the dorsal nerve of the penis, where it is well integrated. While this allowed us to count absolute numbers of nerve fibers, that certainly belonged to the dorsal nerve of the penis, hormone dependent plasticity may instead remodel more distal branches of dorsal nerve fibers or dendrites of sensory neurons in the spinal dorsal horn. In a similar vein Komisaruk and colleagues demonstrated that estrogens can induce functional plasticity of response properties of genital afferents in female rodents (Komisaruk, Adler, & Hutchison, 1972).

Recent studies revealed plasticity of genital somatosensory cortex. Due to the hormone dependent expansion of genital cortex during puberty (Lenschow et al., 2017) and its cellular remodeling (Sigl-Glöckner et al., 2019), we asked if there is a similar change to be observed in the periphery. We reason that the pubertal increase of the cortical magnification of the penis implies and reflects a larger functional relevance of the penis after puberty. However, careful quantification of nerve fibers belonging to the proximal part of the dorsal nerve of the penis did not reveal a difference between prepubertal and adult mice. This is surprising, given that the primary somatosensory cortex is thought to represent the density of sensory fibers in the skin. Hence, the expansion of the genital region observed by Lenschow et al. (2017) might be independent of the density of nerve fibers in the genitals. At the same time, this notion suggests that the cortical magnification (cortical area per penile fiber) of penile fibers increases during puberty. Therefore, we also performed an ad hoc assessment of the cortical magnification of penis nerve fibers and compared it to the cortical magnification of fibers innervating the C2 whisker (as quantified by Welker & Van der Loos, 1986). Specifically, we calculated the ratio between peripheral fibers and the cortical area devoted to the penis or C2 whisker in the somatosensory cortex. This observation suggests that (1) penile fibers are less magnified in somatosensory cortex compared to C2 fibers. At the same time, our previous findings suggest that this magnification might increase for

the genital but not for other body parts during puberty (Lenschow et al., 2017). To fully appreciate the large magnification of certain body parts such as the whisker pad one needs to also consider the 'minimization' of certain body parts such as the leg in the cortical somatosensory representation. We argue that the larger cortical magnification of an afferent in the whisker system reflects a larger functional relevance of cortical processing of whisker afferents than of penile afferents. However, few caveats have to be taken into account interpreting these findings: First, the dorsal penile nerve is a mixed nerve, which contains numerous descending fibers, whereas the C2 whisker fibers quantified by Welker and Van der Loos (1986) were purely sensory. Thus, it may not be surprising that sensory fibers are more extensively represented in sensory cortex. In addition, it may be the case that C2 whisker fibers project more selectively to the somatosensory cortex, whereas penis fibers heavily project to subcortical centers controlling sexuality. To further investigate the relationship of periphery and cortex in the genital system, further experiments are needed, in which both, peripheral innervation and genital cortex size are quantified simultaneously.

In summary, our results suggest that there is no difference in fiber counts in the dorsal nerve of the penis between pre- and post-pubertal mice, despite a significant increase in the size of the penis.

#### ACKNOWLEDGMENTS

We thank Ann Clemens, Jean Simmonet, Constanze Lenschow, and Andreea Neukirchner for comments on the manuscript and Undine Schneeweiß and Tanja Wölk for outstanding technical assistance. We also thank Carsten Lüter and Jutta Zeller from Naturkundemuseum, Berlin for assistance in tissue preparation. This work was supported by Humboldt-Universität zu Berlin, BCCN Berlin (German Federal Ministry of Education and Research BMBF, Förderkennzeichen 01GQ1001A), a grant from the DFG (BR 3479/11-1), NeuroCure, the Gottfried Wilhelm Leibniz Prize of the DFG.

#### CONFLICT OF INTEREST

All authors declare they have no conflict of interest.

#### AUTHOR CONTRIBUTIONS

All authors had full access to all the data in the study and take responsibility for the integrity of the data and the accuracy of the data analysis. Study concept and design: L.P., J.S.G., M.B. Acquisition of data: L.P. Analysis and interpretation of data: L.P., J.S.G., M.B. Drafting of the manuscript: L.P., J.S.G., M.B. Statistical analysis: L.P., J.S.G. Obtained funding: M.B. Administrative, technical, and material support: M.B. Study supervision: M.B.

#### DATA AVAILABILITY STATEMENT

The data in the manuscript will be made available upon request to the corresponding author.

#### ORCID

Michael Brecht  <https://orcid.org/0000-0002-5387-0953>

#### REFERENCES

- Adler, N. T., Davis, P. G., & Komisaruk, B. R. (1977). Variation in the size and sensitivity of a genital sensory field in relation to the estrous cycle in rats. *Hormones and Behavior*, 9(3), 334–344. [https://doi.org/10.1016/0018-506X\(77\)90068-X](https://doi.org/10.1016/0018-506X(77)90068-X)
- Bronson, F. H., & Maruniak, J. A. (1975). Male-induced puberty in female mice: Evidence for a synergistic action of social cues. *Biology of Reproduction*, 13(1), 94–98. <https://doi.org/10.1095/biolreprod13.1.94>
- Calaresu, F. R. (1970). Experimental studies on the dorsal nerve of the penis of the rat. *American Journal of Anatomy*, 127(4), 415–421. <https://doi.org/10.1002/aja.1001270406>
- Carrier, S., Zvara, P., Nunes, L., Kour, N. W., Rehman, J., & Lue, T. F. (1995). Regeneration of nitric oxide synthase-containing nerves after cavernous nerve neurotomy in the rat. *The Journal of Urology*, 153(5), 1722–1727. [https://doi.org/10.1016/S0022-5347\(01\)67512-8](https://doi.org/10.1016/S0022-5347(01)67512-8)
- Chen, Y. L., Chao, T. T., Wu, Y. N., Chen, M. C., Lin, Y. H., Liao, C. H., ... Chiang, H. S. (2018). NNOS-positive minor-branches of the dorsal penile nerves is associated with erectile function in the bilateral cavernous injury model of rats. *Scientific Reports*, 8(1), 1–10. <https://doi.org/10.1038/s41598-017-18988-2>
- Colombel, M., Droupy, S., Paradis, V., Lassau, J. P., & Benoît, G. (1999). Caverno-pudendal nervous communicating branches in the penile hilum. *Surgical and Radiologic Anatomy*, 21(4), 273–276. <https://doi.org/10.1007/s00276-999-0273-9>
- Diamond, J., & Jolly, A. (2018). *Why is sex fun?: the evolution of human sexuality*. Recorded Books.
- Drickamer, L. C., & Murphy, R. X. (1978). Female mouse maturation: Effects of excreted and bladder urine from juvenile and adult males. *Developmental Psychobiology*, 11(1), 63–72. <https://doi.org/10.1002/dev.420110110>
- Feldman, D. E., & Brecht, M. (2005). Map plasticity in somatosensory cortex. *Science*, 310, 810–815.
- Glazewski, S., & Fox, K. (1996). Time course of experience-dependent synaptic potentiation and depression in barrel cortex of adolescent rats. *Journal of Neurophysiology*, 75(4), 1714–1729. <https://doi.org/10.1152/jn.1996.75.4.1714>
- Han, S. H., & Lee, S.-H. (2014). Differential growth of the reproductive organs during the peripubertal period in male rats. *Development & Reproduction*, 17(4), 469–475. <https://doi.org/10.12717/dr.2013.17.4.469>
- Herbert, J. (1973). The role of the dorsal nerves of the penis in the sexual behaviour of the male rhesus monkey. *Physiology and Behavior*, 10(2), 293–300. [https://doi.org/10.1016/0031-9384\(73\)90313-2](https://doi.org/10.1016/0031-9384(73)90313-2)
- Honjin, R., Sakato, S., & Yamashita, T. (1977). Electron microscopy of the mouse optic nerve: A quantitative study of the total optic nerve fibers. *Archivum Histologicum Japonicum = Nihon Soshikigaku Kiroku*, 40(4), 321–332.
- Juraska, J. M., Sisk, C. L., & DonCarlos, L. L. (2013). Sexual differentiation of the adolescent rodent brain: Hormonal influences and developmental mechanisms. *Hormones and Behavior*, 64(2), 203–210. <https://doi.org/10.1016/j.yhbeh.2013.05.010>
- Komisaruk, B. R., & Conde, D. R. (2012). A neuroanatomical correlate of sensorimotor recovery in response to repeated vaginocervical stimulation in rats. *Frontiers in Physiology*, 3, 100.
- Komisaruk, B. R., Adler, N. T., & Hutchison, J. (1972). Genital sensory field: enlargement by estrogen treatment in female rats. *Science*, 178(4067), 1295–1298.
- Larsson, K., & Södersten, P. (1973). Mating in male rats after section of the dorsal penile nerve. *Physiology & Behavior*, 10(3), 567–571. [https://doi.org/10.1016/0031-9384\(73\)90223-0](https://doi.org/10.1016/0031-9384(73)90223-0)
- Lauer, S. M., Lenschow, C., & Brecht, M. (2017). Sexually selected size differences and conserved sexual monomorphism of genital cortex. *Journal of Comparative Neurology*, 525(12), 2706–2718. <https://doi.org/10.1002/cne.24237>

- Lee, K. J., & Woolsey, T. A. (1975). A proportional relationship between peripheral innervation density and cortical neuron number in the somatosensory system of the mouse. *Brain Research*, 99(2), 349–353. [https://doi.org/10.1016/0006-8993\(75\)90035-9](https://doi.org/10.1016/0006-8993(75)90035-9)
- Lenschow, C., Copley, S., Gardiner, J. M., Talbot, Z. N., Vitenzon, A., & Brecht, M. (2016). Sexually monomorphic maps and dimorphic responses in rat genital cortex. *Current Biology*, 26(1), 106–113. <https://doi.org/10.1016/j.cub.2015.11.041>
- Lenschow, C., Sigl-Glöckner, J., & Brecht, M. (2017). Development of rat female genital cortex and control of female puberty by sexual touch. *PLoS Biology*, 15(9), 1–22. <https://doi.org/10.1371/journal.pbio.2001283>
- Levin, R. N., & Johnston, R. E. (1986). Social mediation of puberty: An adaptive female strategy? *Behavioral and Neural Biology*, 46(3), 308–324.
- Liao, Z., & Smith, P. G. (2011). Adaptive plasticity of vaginal innervation in term pregnant rats. *Reproductive Sciences*, 18(12), 1237–1245. <https://doi.org/10.1177/1933719111410706>
- Mucignat-Caretta, C., Caretta, A., & Cavaggioni, A. (1995). Acceleration of puberty onset in female mice by male urinary proteins. *The Journal of Physiology*, 486(2), 517–522. <https://doi.org/10.1113/jphysiol.1995.sp020830>
- Phillips, T. R., Wright, D. K., Gradie, P. E., Johnston, L. A., & Pask, A. J. (2015). A comprehensive atlas of the adult mouse penis. *Sexual Development*, 9(3), 162–172. <https://doi.org/10.1159/000431010>
- Rea, P. (2016). Essential clinically applied anatomy of the peripheral nervous system in the head and neck. In *Essential Clinically Applied Anatomy of the Peripheral Nervous System in the Head and Neck*. Cambridge: Academic Press. <https://doi.org/10.1016/C2014-0-05021-6>
- Sandell, J. H., & Peters, A. (2001). Effects of age on nerve fibers in the rhesus monkey optic nerve. *Journal of Comparative Neurology*, 429(4), 541–553. [https://doi.org/10.1002/1096-9861\(20010122\)429:4<541::AID-CNE3>3.0.CO;2-5](https://doi.org/10.1002/1096-9861(20010122)429:4<541::AID-CNE3>3.0.CO;2-5)
- Schulz, K. M., & Sisk, C. L. (2016). The organizing actions of adolescent gonadal steroid hormones on brain and behavioral development. *Neuroscience and Biobehavioral Reviews*, 70, 148–158. <https://doi.org/10.1016/j.neubiorev.2016.07.036>
- Sigl-Glöckner, J., Maier, E., Takahashi, N., Sachdev, R., Larkum, M., & Brecht, M. (2019). Effects of sexual experience and puberty on mouse genital cortex revealed by chronic imaging. *Current Biology*, 29(21), 3588–3599. <https://doi.org/10.1016/j.cub.2019.08.062>
- Terasawa, E., & Kurian, J. R. (2012). Neuroendocrine mechanism of puberty. In *Handbook of Neuroendocrinology* (pp. 433–484). Cambridge: Academic Press. <https://doi.org/10.1016/B978-0-12-375097-6.10019-8>
- Tomova, A., Deepinder, F., Robeva, R., Lalabonova, H., Kumanov, P., & Agarwal, A. (2010). Growth and development of male external genitalia: A cross-sectional study of 6200 males aged 0 to 19 years. *Archives of Pediatrics and Adolescent Medicine*, 164(12), 1152–1157. <https://doi.org/10.1001/archpediatrics.2010.223>
- Vandenbergh, J. G. (1983). *Pheromonal regulation of puberty. Pheromones and reproduction in mammals*, 95–112. Chicago <https://doi.org/10.1016/b978-0-12-710780-6.50010-8>
- Weech, D., & Ashurst, J. V. (2019). Anatomy, abdomen and pelvis, penis dorsal nerve, *StatPearls*. Retrieved from <http://www.ncbi.nlm.nih.gov/pubmed/30247841>.
- Welker, E., & Van der Loos, H. (1986). Quantitative correlation between barrel-field size and the sensory innervation of the whiskerpad: A comparative study in six strains of mice bred for different patterns of mystacial vibrissae. *The Journal of Neuroscience: The Official Journal of the Society for Neuroscience*, 6(11), 3355–3373. <https://doi.org/10.1523/JNEUROSCI.06-11-03355.1986>
- Yucel, S., & Baskin, L. S. (2003). Identification of communicating branches among the dorsal, perineal and cavernous nerves of the penis. *Journal of Urology*, 170(1), 153–158. <https://doi.org/10.1097/01.ju.0000072061.84121.7d>
- Zoubina, E. V., Fan, Q., & Smith, P. G. (1998). Variations in uterine innervation during the estrous cycle in rat. *Journal of Comparative Neurology*, 397(4), 561–571. [https://doi.org/10.1002/\(SICI\)1096-9861\(19980810\)397:4<561::AID-CNE8>3.0.CO;2-#](https://doi.org/10.1002/(SICI)1096-9861(19980810)397:4<561::AID-CNE8>3.0.CO;2-#)

**How to cite this article:** Purkart L, Sigl-Glöckner J, Brecht M. Constant innervation despite pubertal growth of the mouse penis. *J Comp Neurol*. 2020;528:2269–2279. <https://doi.org/10.1002/cne.24892>